TECHNICAL REPORT 4213

NEW INSTRUMENTATION FOR THE LIGHT OUTPUT MEASUREMENT OF PHOTOFLASH ITEMS

LOUIS R. SZABO

JUNE 1971

PICATINNY ARSENAL
DOVER, NEW JERSEY

UNCLASSIFIED
Security Classification

DOCUMENT CONTROL DATA - R & D

(Security classification of title, body of abstract and indexing annotation must be entered when the overall report is classified)

1. ORIGINATING ACTIVITY (Corporate author)

Picatinny Arsenal, Dover, N. J. 07801

2a. REPORT SECURITY CLASSIFICATION

UNCLASSIFIED

2b. GROUP

3. REPORT TITLE

NEW INSTRUMENTATION FOR THE LIGHT OUTPUT MEASUREMENT OF PHOTOFLASH ITEMS

4. DESCRIPTIVE NOTES (Type of report and inclusive dates)

5. AUTHOR(S) (First name, middle initial, last name)

Louis R. Szabo

6. REPORT DATE	7a. TOTAL NO. OF PAGES	7b. NO. OF REFS
JUNE 1971	35	2

8a. CONTRACT OR GRANT NO.	9a. ORIGINATOR'S REPORT NUMBER(S)
b. PROJECT NO.	Technical Report 4213
c. AMCMS Code 4810.16.4104.8	9b. OTHER REPORT NO(S) (Any other numbers that may be assigned this report)
d.	

10. DISTRIBUTION STATEMENT

Approved for public release; distribution unlimited

11. SUPPLEMENTARY NOTES	12. SPONSORING MILITARY ACTIVITY

13. ABSTRACT

The major problem of measuring candlepower always has been associated with the use of properly corrected phototransducers. Many manufacturers of photodetectors claim to have cells corrected to the equivalent spectral response of the human eye, however, investigations of all these so-called corrected cells revealed that their correction to the ICI response is very crude. Only one manufacturer produces a cell with an acceptable correction, but it has limitations in time response, stability, and shelf life.

It is therefore, a significant and necessary accomplishment to develop a light sensor which has an accurate and reproducible ICI correction, fast rise time, stability, and long shelf life. The project which is the subject of this report has accomplished these objectives.

An accurate, low cost integrator also was developed in this program. It provides for the first time, a device which is specifically suited for use by all manufacturers of military light producing items.

DD FORM 1 NOV 68 1473 REPLACES DD FORM 1473, 1 JAN 64, WHICH IS OBSOLETE FOR ARMY USE.

UNCLASSIFIED
Security Classification

14 KEY WORDS	LINK A		LINK B		LINK C	
	ROLE	WT	ROLE	WT	ROLE	WT
Integrator, light, digital						
Integrator, light, analog						
Transducer, candlepower						
Light sensors						
ICI correction						
Rise time						
Silicon photovoltaic cell						

Technical Report 4213

NEW INSTRUMENTATION FOR THE LIGHT OUTPUT MEASUREMENT OF PHOTOFLASH ITEMS

by

Louis R. Szabo

JUNE 1971

AMCMS Code 4810.16.4104.8

Pyrotechnics Laboratory
Feltman Research Laboratories
Picatinny Arsenal
Dover, N.J.

The citation in this report of the trade names of commercially available products does not constitute official indorsement or approval of the use of such products.

ACKNOWLEDGEMENTS

The author wishes to acknowledge the valuable advice of Mr. M. Lazarus in the development of the digital panel integrator, and the experimental and analytical work done by Mr. R. Frisina, which helped to accomplish the breakthrough in the development of the corrected photocell.

His appreciation is extended also to Mr. J. Knutelsky for his skillful assistance in the laboratory work.

TABLE OF CONTENTS

	Page No.
Abstract	1
Introduction	2
Development	3
Candlepower Light Detector	3
Gated Light Integrator	8
Discussion of Results	10
References	12
Distribution List	30
Tables	
1 Silicon photovoltaic cell output	13
2 Test results on standard colored filters	14
3 Comparison of integrator performance using square wave pulse for signal source	15
4 Deviation from linearity vs illumination and load resistance	16
5 Performance evaluation of the digital panel integrator	17
Figures	
1 Relative spectral response of the human eye	18
2 Typical relative spectral response of a silicon photovoltaic cell	19

3	Equivalent circuit of the photovoltaic cell	20
4	Internal resistance vs illumination	21
5	Output variation vs temperature	22
6	Relative transmission function of the ideal correction filter	23
7	Family of transmission curves vs glass thickness	24
8	Relative spectral response of the new corrected silicon sensor vs the idea $\bar{y}$ function	25
9	Block diagram of the analog integrator system	26
10	The light output of a typical photoflash	27
11	Trigger circuit for the digital panel integrator	28
12	Linearity curves of silicon photocells vs light level and load	29

ABSTRACT

The major problem of measuring candlepower always has been associated with the use of properly corrected phototransducers. Many manufacturers of photodetectors claim to have cells corrected to the equivalent spectral response of the human eye; however, investigations of all these so-called corrected cells revealed that their correction to the ICI response is very crude. Only one manufacturer produces a cell with an acceptable correction, but it has limitations in time response, stability, and shelf life.

It is therefore, a significant and necessary accomplishment to develop a light sensor which has an accurate and reproducible ICI correction, fast rise time, stability, and long shelf life. The project which is the subject of this report has accomplished these objectives.

An accurate, low cost integrator also was developed in this program; it provides, for the first time, a device which is specifically suited for use by all manufacturers of military light producing items.

INTRODUCTION

The proper exposure of a film emulsion depends on the quantity of light it receives, which, in turn, is determined by the time integral of the luminous flux that can be expressed in candleseconds. Specifications on photoflash items, as used in aerial photography, are given in terms of total light (candleseconds) for a duration of 40 milliseconds. The testing of these items requires, therefore, a true candlepower measuring transducer and a gated integrator.

At present the 929 photoemissive vacuum tube, which has an S4 response, is being used. Its correction to the human eye response is very poor and requires a power supply which degrades its stability. The 856 Weston photovoltaic sensor, which has an acceptable ICI correction, was recently considered for these measurements; however, its slow time response precludes its use for this application.

For many years the total light integral was hand evaluated in the following manner: The light transducer was connected to an oscilloscope and a time vs intensity curve was recorded by taking a polaroid picture of each item, which then was integrated manually by means of a planimeter. This is a time-consuming, highly inaccurate operation. Scope gain offset, time base offset, line thickness on picture, and the evaluator's judgment can all contribute to error. Based on past experience, this inaccuracy can run as high as 20%.

Several years ago various types of integrators were tried for use in photoflash work; however, the state-of-the-art of electronics at that time precluded the development and use of a field instrument, so that those integrators were not a substantial improvement over the manual method.

The need for a foolproof automatic light integrator became more and more obvious as time went on. Early in this program an analog integrator was designed and tested. It performed well; however, its calibration and operation was cumbersome, and its cost relatively high, an estimated $2,200 for a dual (two-channel) instrument. In the search for an improved method, attention was shifted to the more modern digital approach. The exploding integrated circuitry technology made available a new 2 1/2 digit panel voltmeter, which was modified to adjust its sampling time to 40 milliseconds. The unit requires only a simple trigger circuit, which consists of a few small

components. Experimental test results with this instrument were excellent, with an actually obtained accuracy of ± .5%. In contrast to the analog intergrator, the operation of this digital integrator is simple: no adjustments are required; its size is miniature (overall dimensions 8 x 8 x 6 inches for a dual two-channel integrator); and the cost is reduced to $800.

DEVELOPMENT

Candlepower Light Detector

A true candlepower transducer is a photoelectric device which converts light energy to electrical current linearly following a specific attenuation function (spectral response) throughout the visible spectrum. This function is that of an average human eye and is called the ICI response, or $\bar{y}\lambda$ function (Fig 1). The transducer has to be linear; i.e., an increased amount of light energy at any given wavelength will result in a proportionally increased current output from the cell.

Since no photodetector with the spectral luminous efficiency of the $\bar{y}\lambda$ function exists, correction is required. It is accomplished by applying a colored glass filter or set of filters to force the detector's response to the desired function. The overall response then is

$$\bar{y}\lambda = D\lambda F\lambda$$

where $D\lambda$ is the detector's relative spectral efficiency, and

$F\lambda$ is the combined relative transmission function of the correction filter.

In general, once the filter requirements are established, reproducibility in mass manufacturing the transducer mostly depends on the spectral uniformity of the photodetectors, that is, when normalized, $D_1\lambda = D_2\lambda \ldots = D_n\lambda$. Transmission characteristics of the filters also might change from melt to melt each time a batch of colored

filter glass is produced by the manufacturer; however, in general compensation can easily be obtained by changing the thickness of the filter. In contrast, the spectral efficiency of a given detector cannot be appreciably changed, since its characteristics are determined by the element used for photon conversion. For these reasons, it is more feasible to first select a detector, and then custom-design the desired filter or filter system.

An evaluation of candidate photodetectors follows, with special attention given to these factors:

Spectral response

Sensitivity

Time constant

Linearity

Stability

Simplicity

The phototube or its improved version, the photomultiplier, is a photoemissive device; that is, the absorption of photons leads to the ejection of electrons. The quantum efficiency of these tubes (ratio of the number of ejected electrons to the number of received photons) is relatively high due to the fact that their internal gain is in excess of the 10^{10} power. They are also superior in rise time. Operation is possible at frequencies as high as 100 Mc. However, they are costly and they require precision high voltage power supplies which are expensive and bulky. The extent of their stability, or the lack of it, is highly dependent on the performance of the power supply. For these reasons, and also considering their fragile structure and large size, photomultipliers were rejected for the application.

The photoconductive semiconductors also were rejected because of their excessive drift vs temperature.

The silicon photovoltaic cell has been selected after thorough study and experimentation. It is a p-n junction semiconductor, also called barrier layer cell, since there is a potential barrier at the

junction. The incident light produces electron-hole pairs, the hole diffusing to the junction, thereby producing current.

Spectral Response

The spectral response of the silicon barrier layer cell is shown in Figure 2. Its quantum efficiency at the shorter wavelengths (violet and blue region) is relatively low; however, this does not constitute a handicap, since the response in this region of the human eye is even lower as indicated in Figure 1. The efficiency peaks at 960 nm and goes to zero at about 1100 nm.

The spectral response of the cells within a manufacturer's lot and among lots must be reasonably consistent; otherwise, an individual ICI correction would be required for each cell. Experiments have been conducted on several photovoltaic sensors made by three different manufacturers. A Bausch and Lomb monochromator was used as a single wavelength source. Calibration for equal energy across the visible spectrum was accomplished by the use of thermopiles. The results are tabulated in Table 1.

The spectral efficiency curves of these items show only slight variations, and for all practical purposes they can be considered uniform.

Sensitivity

The sensitivity of the silicon photocell is 0.275 microamperes per footcandle per square centimeter, which is 3.12 times better than that of the selenium cell.

Time Constant

The low time constant or rise time of the silicon barrier layer cell is also a great improvement over the selenium cell. The rise time of selenium at illumination levels of one footcandle or higher is approximately five milliseconds. At lower light levels the rise time increases, however, to several minutes, and for the optical measurement of low light levels, or short duration photoflash items, the selenium barrier layer cell is useless.

The silicon cell, on the other hand, has a time constant on the order of a few microseconds, with a slight degradation at very low illumination levels. It therefore suits photoflash items which have rise times on the order of one millisecond.

Linearity

Linearity is a function of the relation between the cell's internal resistance R_p and the load resistance R_l (Fig 3). The undesirable internal resistance R_p provides a leakage path for the generated current, which could be easily compensated for if it were a constant. However, it varies with the illumination level as shown in Figure 4. A one percent or better accuracy in linearity can be achieved, provided that the realtion

$\frac{R_p}{R_l} = 100$ is maintained. Note that R_s, a constant internal resistance, is in series with R_l; however, judging from experimental results, it is negligible.

As an example, if the expected maximum illumination level on a given cell (Fig 4) is 10 footcandles

$$R_l = \frac{R_p}{100} = \frac{100,000}{100} = 1000 \text{ ohms maximum.}$$

By knowing the sensitivity of the photocells (0.275 microamperes per footcandle per square centimeter), we also know that for the desired one percent accuracy our maximum output ($I_l R_l$) should not be higher than 2.75 millivolts. This is a valuable safeguard against erroneous results.

Stability

Stability vs time was found excellent; more than 40 cells showed no noticeable change through a time period of one year. The stability vs temperature data is shown on Figure 5. The temperature coefficient is 0.0825 percent per degree F.

The relative transmission function of the required correction filter for the silicon cell can be resolved from equation

$$F_\lambda = \frac{\bar{y}_\lambda}{D_\lambda} \quad \text{as shown in Figure 6.} \qquad (2)$$

An attempt was made to design an interference filter to match F_λ but it proved to be unsuccessful because of a sharp cutoff. The high cost of these filters also made them undesirable.

The transmission functions of colored glass filters are more readily changeable, since their attenuation slope can be changed by changing the thickness of the glass. It was found, however, that no single filter could match F_λ.

The combined transmission characteristics of Corning Glass Filters 3780 and 9788 appeared to be the best approximation to match the desired curve F_λ. A consultation with Corning Glass scientists revealed, however, that Glass 9788 is a special filter, and as such its characteristics are not as well controllable as those of other glass filters. At the standard 5 mm thickness, the transmission of various melts (manufacturing units) can vary widely; furthermore, a melt yields only two to three 6 1/2 inch square plates.

Corning Glass Works supplied the data for study on a wide variety of 9788 melts manufactured throughout the years. A logarithmic equation also was provided to compute transmission changes as a result of changing the glass thickness.

$$T_\lambda = K\ 10^{-B_\lambda t} \qquad (3)$$

$$B_\lambda = \frac{\log K - \log T_\lambda}{t} \qquad \text{or} \qquad (4)$$

$$t = \frac{\log K - \log T_\lambda}{B_\lambda} \qquad (5)$$

where T_λ is the transmission of the filter at the particular wavelength

K is the surface reflectance factor and given as 0.9216

t is the thickness of the glass

B_λ is the glass index of the particular melt at the particular wavelength.

(Any measuring unit may be used, but its use must be consistent throughout the computation.)

Equation (3) is very valuable for generating a family of transmission curves as a function of thickness (see Fig 7). The calculating procedure is as follows:

Given: The spectral transmission curve for the filter in question.

1. Compute B for wavelengths which are of interest, using Equation (4).

2. Compute the transmissions for different thicknesses or the thickness for the desired transmission, using Equations (3) and (5), respectively, as desired.

Using Equations (3), (4), and (5), approximately 50 different melts of 9788 filters have been analyzed analytically. The majority of the melts was found to be satisfactory to match the red cutoff portion of ideal response curve F_λ (Fig 6), if each of them were to be ground to a specific critical thickness. The left or blue cutoff portion of the curve can easily be matched by Filter 3780 at 1.2 mm thickness.

The combined spectral response of the silicon photovoltaic cell and colored glass filters 3780 and 9788 is shown in Figure 8, as well as the ICI or eye response curve $\bar{y}_\lambda$ for comparison.

Gated Light Integrator

Photoflash specifications call for a certain integrated light energy which is derived from the exposure requirements of the film. The time interval is directly related to the duration of the camera's shutter

opening, and it is set at 40 milliseconds. Therefore, to test photoflash items a gated 40 millisecond light integrator is required. The integrator must trigger on first light, integrate for 40 milliseconds, then shut off and hold the value until it is reset. The integral is expressed in candleseconds.

The system presently used consists of an oscilloscope with a camera which records a time-intensity curve. Integration is done manually by using a planimeter on these curves. This operation is not only time-consuming but also highly unreliable. In the light of modern technology, the design of a new automatic system became imperative. Considerations were given to both analog and digital integrators.

However, the multi-thousand dollar cost of a commercial integrating digital voltmeter was considered prohibitive. A hybrid analog integrator module has been purchased and evaluated. On the basis of the promising test results (accuracy, time response, etc), an analog integrator system with a digital readout has been designed and fabricated.

The block diagram of the integrator is shown in Figure 9. It functions as follows: At time t_0 (Fig 10) photoflash is ignited. A few microseconds later t_{0+} trigger circuit resets integrator and places an initial condition on the integrator if desired. One-hundred microseconds later at $t_{.1}$, the delay circuit triggers the 40 millisecond timer. At the same time the 40 millisecond timer activates the electronic switch in the integrator which connects the signal cell to the integrator input. Integration is in progress. The 40 millisecond clock sends out a positive 40 millisecond wide pulse. At the falling edge t_{40} the Schmidt trigger sends a 10 microsecond wide pulse to the digital panel meter, a command to make a readout. The integral appears on the meter and will stay there until the system is reset. As a result, any leakage or drift in the integrator will not affect the numerical readout and will not introduce error.

It should be noted that the integrator has a built-in, foolproof check regarding offsets and precise accuracy of the 40 millisecond duration. Its accuracy is comparable to that of a very expensive commercial digital integrator.

While this phase of the project was under way, new low priced sophisticated digital panel meters were put on the market. In view of the relatively high cost of the analog integrator system (approximately $2,500 for a dual integrator), a new study was launched to find the feasibility of modifying the small panel meters to perform the gated integration.

The small digital panel meters were designed to measure DC voltage levels. Their IC preamplifiers are low performance type, highly filtered, which result in a very slow rise time. Their sampling rate is approximately 17 milliiseconds derived from the 60 cps line frequency.

A 100 millivolt full scale digital panel meter was purchased for experimentation. The sampling rate was easily changed to 40 milliseconds by replacing the original synchro-multivibrator with an independent hybrid "one shot". The automatic readout also was inactivated, and an external trigger circuit added (Fig 11), which triggers the instrument on first light. A readout will appear 40 milliseconds later and will stay until the next trigger signal enters.

Filtering was reduced in order to increase time response. Test results were consistently low, which indicated a still slow rise time. Filters were removed and the input was carefully shielded to reduce or prevent AC noise. This modification improved the accuracy to ± 1/2 %, compared with Vidar's Model 260 sophisticated integrating voltmeter.

The cost of a two-channel digital channel integrator system is approximately $800, or about 1/3 that of the analog integrator system.

DISCUSSION OF RESULTS

A crude method, called the Three Color Check, is being used at present as an acceptance criterion of Weston's 856 selenium candlepower sensors. It consists of three selected NBS certified standard filters (Corning's 4407A, 3480A, and 2412C colored glasses, bluish green, yellow, and red, respectively), each with a known luminous flux attenuation number. The light source must be a tungsten filament lamp operated at 2854°K color temperature. The tolerance is

set at ± 5 %; that is if, for instance, the rated transmission is 23.2%, the output of the sensor, when the colored filter is applied, must fall between 22.04 and 24.36% of the signal obtained without the colored filter.

The prototype sensor was tested on several colored glass filters with dominant wavelengths across the visible spectrum. All data (shown in Table 2) fell within the allowed tolerances.

The more representative, accurate, point by point spectral response of the new sensor also was obtained. Used was the Bausch and Lomb Model 102-49 Monochromator with known energy output at each wavelength. The result was highly satisfactory. The filter correction on the silicon cell produced a better match to the eye response than that of the corrected 856 Weston selenium cell. The curves are shown for comparison in Figure 8.

The linearity test also was conducted on the new sensor. It is important to know the limitations of the transducer, since errors due to overload are not apparent. The experiment was conducted by exposing the sensor to a known illumination level and measuring its signal outputs under various load conditions. In other words, the output signal is equal to the product of cell current and load resistor: $v_o = I_c R_l$. Since we know that the cell current is 1.4 microamperes per footcandle, the output signal should be 1.4 R_l microvolts per footcandle. For instance, if the illumination is 100 footcandles and the load resistance 100 ohms, the output signal should be 14.00 millivolts. As shown in Table 4, the experimental value is 13.96 millivolts, a deviation of about 0.3%. There is a convenient built-in safeguard against overload in the device. As an example, if we want 1% accuracy and have a 100 ohm load resistor, we know from Table 4 that our maximum signal output must not exceed 112 millivolts.

A graphical expression of Table 4 is given in Figure 12. Both the analog and digital integrators were tested for time response and accuracy.

First, a single pulse square wave generator was used with variable but known amplitude and width. The generator was triggered with a delay, variable from 0 to 10 milliseconds. This was necessary to be able to detect a possible undesirable delay in the integrator's trigger circuits. Integrals were taken simultaneously with the

analog, digital, and Vidar's integrating voltmeter. The former is a highly accurate, multi-purpose commercial device; it was used for reference in comparing results. Test results are tabulated in Table 3. Each number represents the average of 5 consecutive instrument readings taken under the same test position. The deviations within any group of five readings were less than 0.2%. The percentage deviations are shown on Table 3 for comparison. Experiments also have been conducted using M3 flashbulbs as a simulative for photoflash items. Results are shown in Table 5.

REFERENCES

1. A. C. Hardy, Handbook of Colorimetry, The Technology Press, Massachusetts Institute of Technology, Cambridge, Massachusetts, 1936

2 Gunter Wyszecki and W. S. Stiles, Color Science, John Wiley and Sons Inc., New York, 1967

TABLE 1

Silicon photovoltaic cell output

(Normalized to 550 nm)

Wavelength (nm)	IRC Model S2900GE9.5M					RCA		TI	
	No. 1	No. 2	No. 3	No. 4	No. 5	No. 1	No. 2	No. 1	No. 2
400	3.6	3.2	3.8	4.6	3.1	3.5	3.7	-	-
410	11.6	11.1	11.9	13.1	11.0	-	-	10.5	10.4
420	18.8	18.5	19.1	19.7	18.2	-	-	-	-
430	25.9	25.0	26.3	26.5	25.4	-	-	24.7	24.7
440	33.9	33.6	34.5	34.7	33.6	-	-	-	-
450	41.1	41.3	41.7	41.9	40.6	40.7	41.5	40.6	40.2
460	48.2	47.9	49.1	49.0	47.4	-	-	-	-
470	52.7	52.5	53.2	53.3	52.0	-	-	52.1	51.9
480	58.9	58.5	59.3	59.6	58.3	-	-	-	-
490	65.0	64.7	65.1	65.8	64.2	-	-	64.5	64.3
500	71.4	71.3	71.6	72.1	70.7	71.7	71.6	-	-
510	76.8	76.5	77.2	77.7	76.1	-	-	76.5	76.4
520	83.0	82.5	84.0	83.7	82.5	-	-	-	-
530	88.4	87.9	88.9	89.0	88.0	-	-	88.3	88.1
540	93.8	94.0	94.5	93.5	93.6	-	-	-	-
550	100.0	100.0	100.0	100.0	100.0	100.0	100.0	100.0	100.0
560	104.5	104.9	105.3	104.7	105.1	-	-	-	-
570	108.9	109.3	109.2	109.0	109.6	-	-	109.1	109.3
580	112.5	113.1	112.9	112.7	112.7	-	-	-	-
590	117.0	118.1	117.5	117.3	117.5	-	-	117.3	117.4
600	121.4	122.3	121.2	121.5	121.9	122.5	123.0	-	-
610	125.0	125.8	124.7	124.9	125.7	-	-	125.6	125.6
620	129.5	130.1	129.0	129.6	130.9	-	-	-	-
630	133.0	133.7	132.3	132.9	133.9	-	-	133.4	133.2
640	136.6	137.1	135.8	136.4	137.4	-	-	-	-
650	141.1	141.8	140.3	140.9	142.0	140.7	141.7	141.0	140.9
660	144.6	144.9	143.9	144.3	145.3	-	-	-	-
670	147.3	147.6	146.7	147.0	148.0	-	-	147.5	147.3
680	150.9	151.3	150.3	150.5	151.7	-	-	-	-
690	153.6	154.1	153.6	153.3	154.2	-	-	154.0	153.7
700	157.1	157.5	157.2	157.4	158.1	158.2	157.6	-	-

TABLE 2

Test results on standard colored filters

Filter No.	Y Stand.	Y Exp.	Deviation %
2412A	13.7	13.54	-1.2
2412B	12.5	12.58	+.64
2412C	13.4	13.04	-2.7
2418A	11.8	11.65	-1.3
2424A	25.7	25.48	-.86
3060A	87.3	86.35	-1.08
3307A	51.0	50.47	-1.04
3384A	77.1	76.61	-.636
3384B	84.9	83.62	-.33
3480A	38.6	37.94	-1.7
3482A	61.2	60.64	-.92
3485A	84.3	84.34	+.04
3486A	77.5	77.90	+.51
3486D	74.0	73.64	-.5
4060C	16.8	17.34	+3.2
4303A	18.3	18.83	+2.9
4303B	17.0	16.80	-1.17
4308A	44.5	45.26	+1.5
4308C	36.3	37.73	+1.2

TABLE 3

Comparison of integrator performances
using square wave pulse for signal source

Input Pulse			Integral			% Deviation From Vidar	
Ampl. mv	Width msec	Delay msec	Vidar mv	Analog volt	Digital mv	Analog %	Digital %
100	5	10	50.1	.498	12.4	.6	1.0
100	20	10	200.0	2.010	49.8	.5	.4
50	10	10	50.0	.496	12.5	.8	0
50	20	10	100.4	1.010	25.2	.6	.3
10	5	10	4.98	.047	*	5.0	*
10	20	10	19.9	.189	*	.5	*
10	5	0	5.01	.048	*	4.2	*
10	20	0	20.0	.199	*	.5	*
10	40	0	40.2	.405	*	.7	*
25	5	0	12.4	.122	*	.2	*
25	10	0	25.0	.248	*	.8	*
25	20	0	50.3	.501	12.6	.4	.2
25	40	0	99.8	1.012	24.9	.1	.2
50	5	0	25.0	.247	*	.1	*
50	10	0	49.9	.497	12.4	.4	.6
50	20	0	100.3	1.015	25.2	.5	.5
50	40	0	199.7	2.013	49.7	.8	.4
100	5	0	50.0	.496	12.3	.8	.2
100	10	0	100.1	1.021	25.1	.2	.3
100	20	0	199.9	2.027	50.1	.1	.3
100	40	0	400.2	4.053	100.5	.1	.5

(*) No usable data was obtained because of the small signal input.

TABLE 4

Deviation from linearity vs
illumination and load resistance

Illum. E (FC)	Load Res. R_1 (OHMS)	OUTPUT V (Exp.) (MV)	OUTPUT V' (Theoret.) (MV)	Diff. V' - V	Dev. (%)
10	50	0.700	0.700	0.000	0.00
10	100	1.3999	1.400	0.001	-0.07
10	200	2.796	2.800	0.004	-0.1
10	300	4.188	4.200	0.012	-0.3
10	400	5.578	5.600	0.022	-0.4
10	500	6.966	7.000	0.034	-0.5
10	600	8.349	8.400	0.051	-0.6
10	700	9.725	9.800	0.075	-0.8
10	800	11.10	11.20	0.10	-0.9
10	900	12.48	12.60	0.12	-1.0
10	1000	13.84	14.00	0.16	-1.1
10	2000	27.42	28.00	0.58	-2.1
10	3000	40.45	42.00	1.55	-3.7
10	4000	52.98	56.00	3.02	-5.4
10	5000	65.00	70.00	5.00	-7.1
10	6000	76.45	84.00	7.55	-9.0
10	7000	87.30	98.00	11.70	-11.9
10	8000	97.48	112.0	14.52	-13.0
10	9000	107.0	126.0	19.0	-15.1
10	10000	115.8	140.0	24.2	-17.3
25	20	0.700	0.700	0.000	0.00
25	40	1.399	1.400	0.001	-0.07
25	60	2.099	2.100	0.001	-0.05
25	80	2.798	2.800	0.002	-0.07
25	100	3.498	3.500	0.002	-0.06
25	200	6.987	7.000	0.013	-0.2
25	400	13.95	14.00	0.05	-0.4
25	600	20.88	21.00	0.12	-0.6
25	800	27.76	28.00	0.24	-0.9
25	1000	34.59	35.00	0.41	-1.2
25	2000	67.96	70.00	2.04	-2.9
25	3000	99.53	105.0	5.47	-5.2
25	4000	128.7	140.0	11.3	-8.1
25	5000	154.3	175.0	20.7	-11.8
50	10	0.700	0.700	0.000	0.00
50	20	1.400	1.400	0.000	0.00
50	40	2.798	2.800	0.002	0.07
50	60	4.197	4.200	0.003	-0.07
50	80	5.597	5.600	0.003	-0.05
50	100	6.989	7.000	0.011	-0.15
50	200	13.96	14.00	0.04	-0130
50	400	27.86	28.00	0.14	-0.55
50	600	41.64	42.00	0.36	-0.9
50	800	55.33	56.00	0.67	-1.3
50	1000	68.87	70.00	1.13	-1.6
100	10	1.400	1.400	0.000	0.00
100	20	2.799	2.800	0.001	-0.03
100	50	6.985	7.00	0.011	-0.15
100	100	13.96	14.00	0.04	-0.3
100	200	27.86	28.00	0.14	-0.5
100	300	41.70	42.00	0.30	-0.7
100	400	55.50	56.00	0.50	-0.9
100	500	69.26	70.00	0.74	-1.1
100	600	82.93	84.00	1.07	-1.3
100	700	96.55	98.00	1.45	-1.5
100	800	110.0	112.0	2.0	-1.8
100	900	123.3	126.0	2.7	-2.2
100	1000	136.5	140.0	3.5	-2.5
200	20	5.600	5.600	0.000	0.00
200	40	11.17	11.20	0.03	-0.2
200	80	22.35	22.40	0.05	-0.2
200	100	27.92	28.00	0.08	-0.3
200	200	55.71	56.00	0.29	-0.5
200	400	110.9	112.0	1.1	-1.0
200	600	164.8	168.0	3.2	-1.9

TABLE 5

Performance evaluation of the digital panel integrator

Integral Output =		Deviation
Vidar	DPM	%
398.0	100.1	.6
360.8	89.5	.8
388.7	97.5	.3
382.4	95.8	.2
392.0	97.7	.5
366.9	92.0	.3
379.5	94.0	.9
380.7	95.4	.2
381.7	96.2	.8
429.2	106.6	.6
388.6	98.1	.8
380.3	95.3	.2
360.0	89.7	.3
388.4	96.8	.3
382.2	95.0	.6

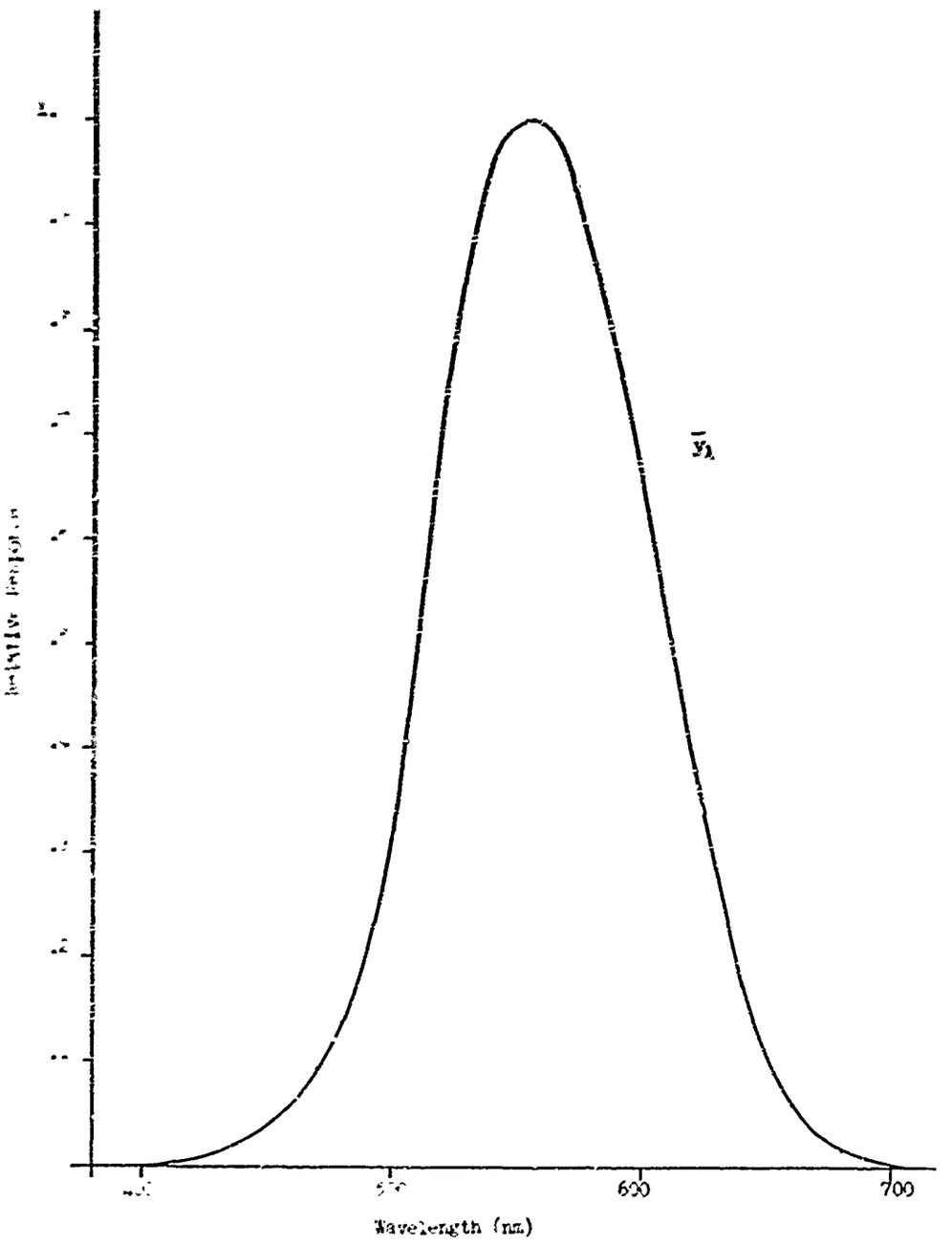

Fig 1 Relative spectral response of the human eye

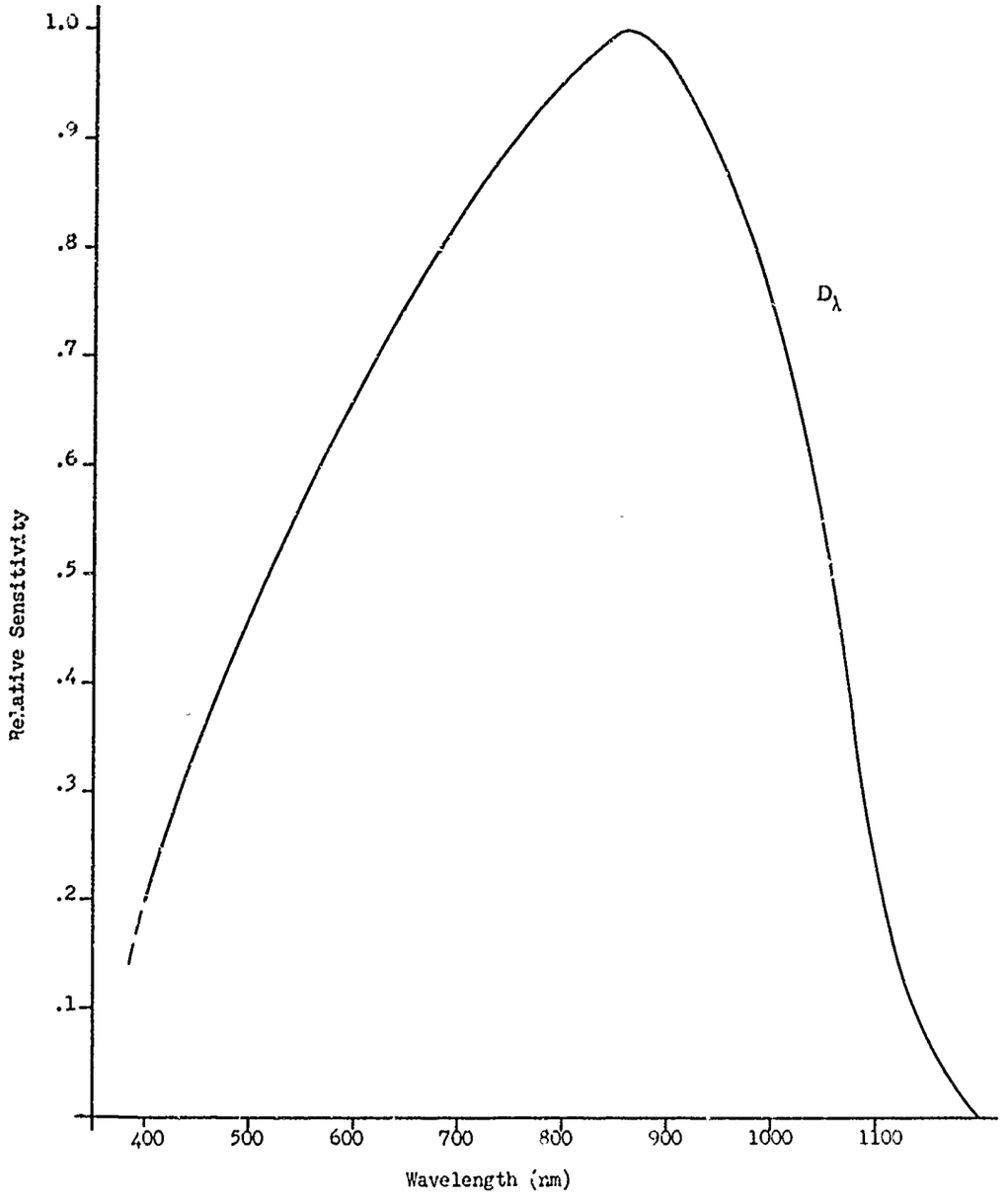

Fig 2 Typical relative spectral response of a silicon photovoltaic cell

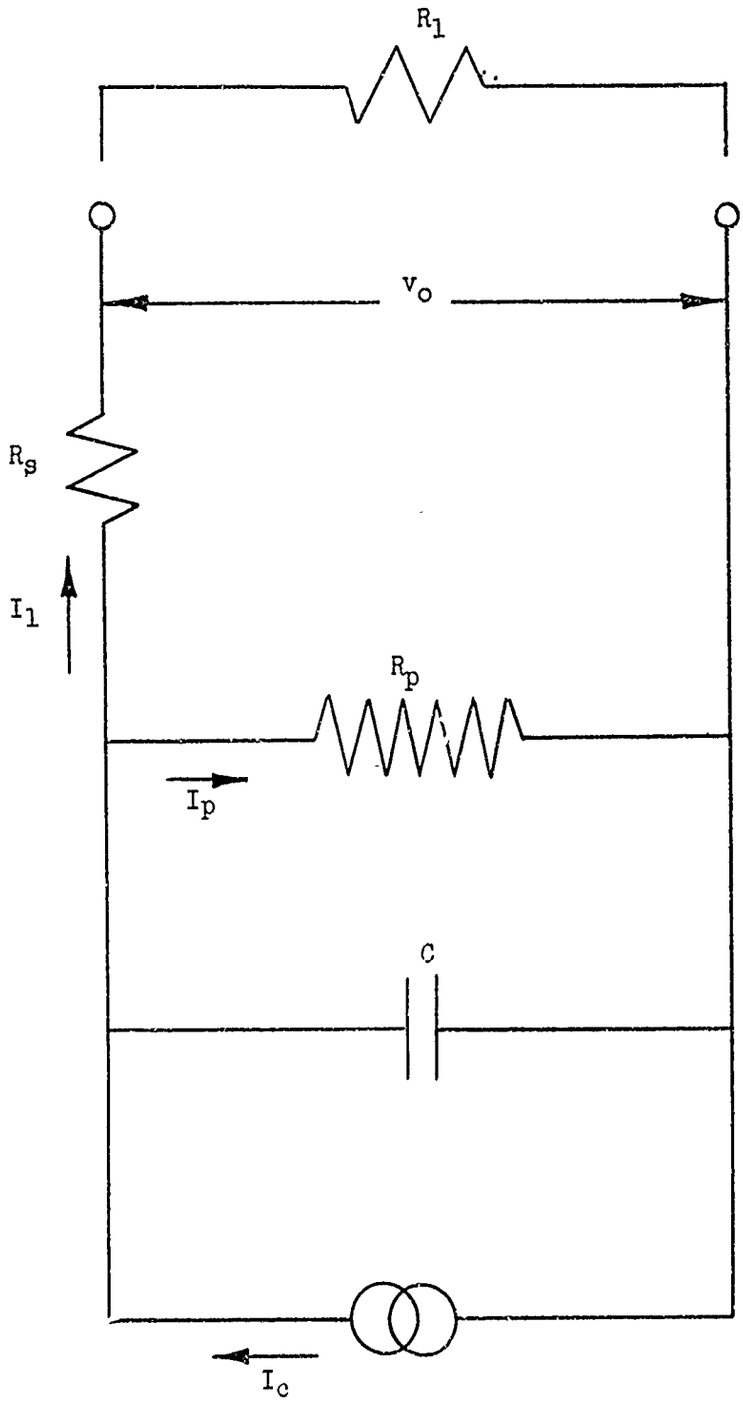

Fig 3 Equivalent circuit of the photovoltaic cell

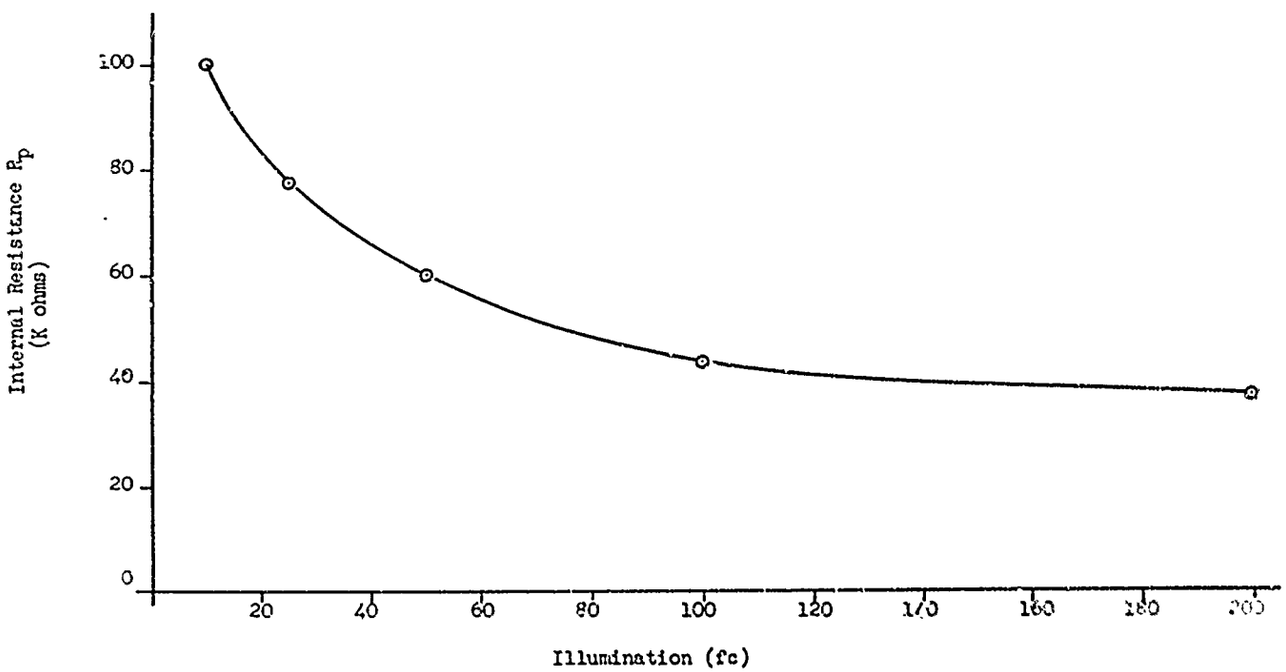

Fig 4 Internal resistance vs illumination

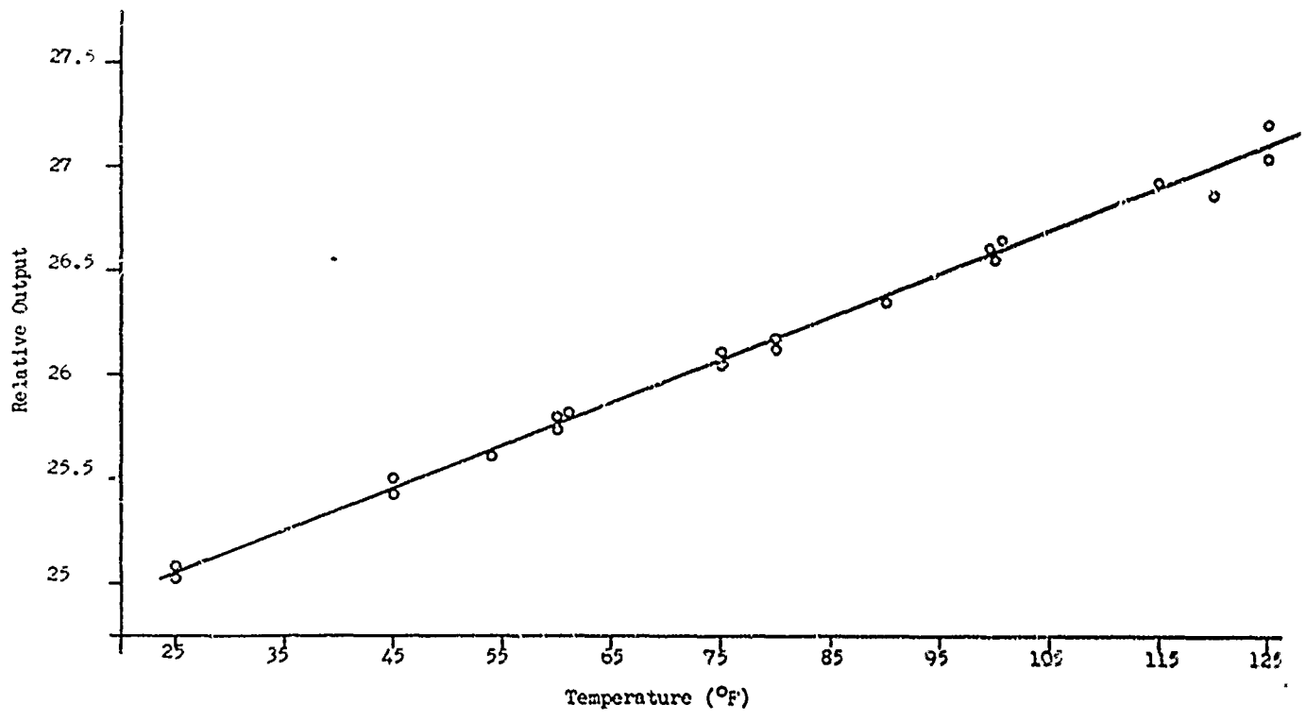

Fig 5 Output variation vs temperature

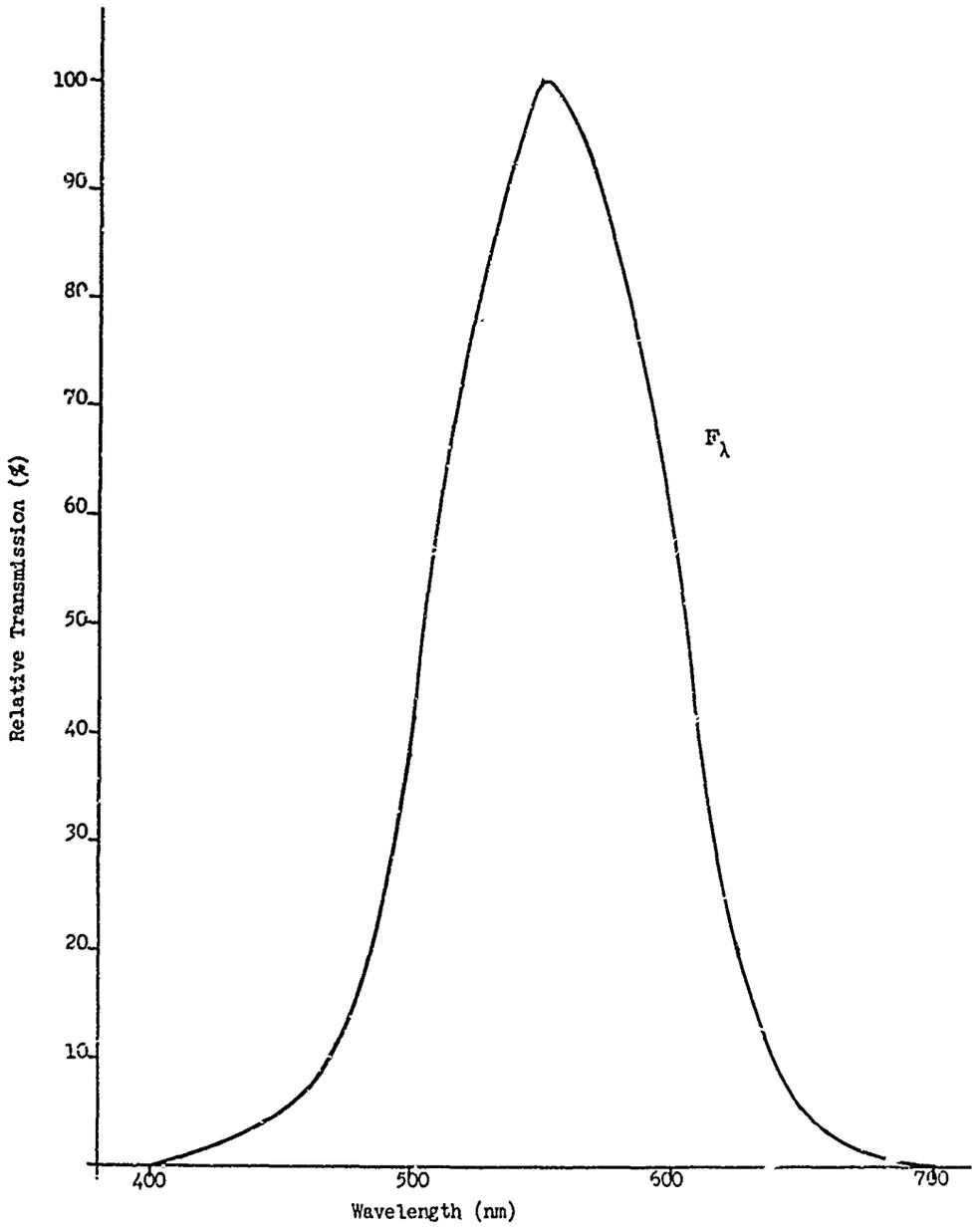

Fig 6 Relative transmission function of the ideal correction filter

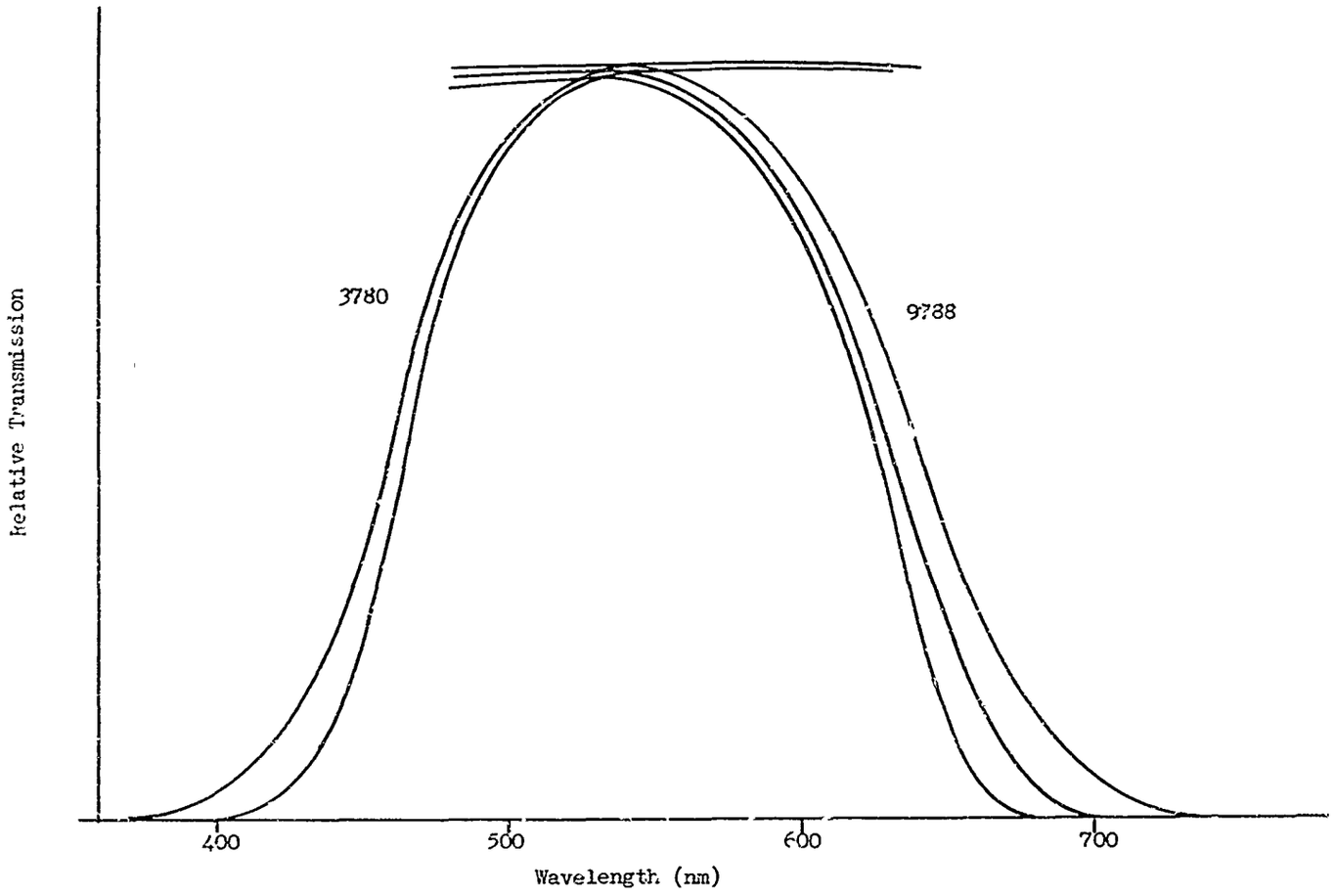

Fig 7 Family of transmission curves vs glass thickness

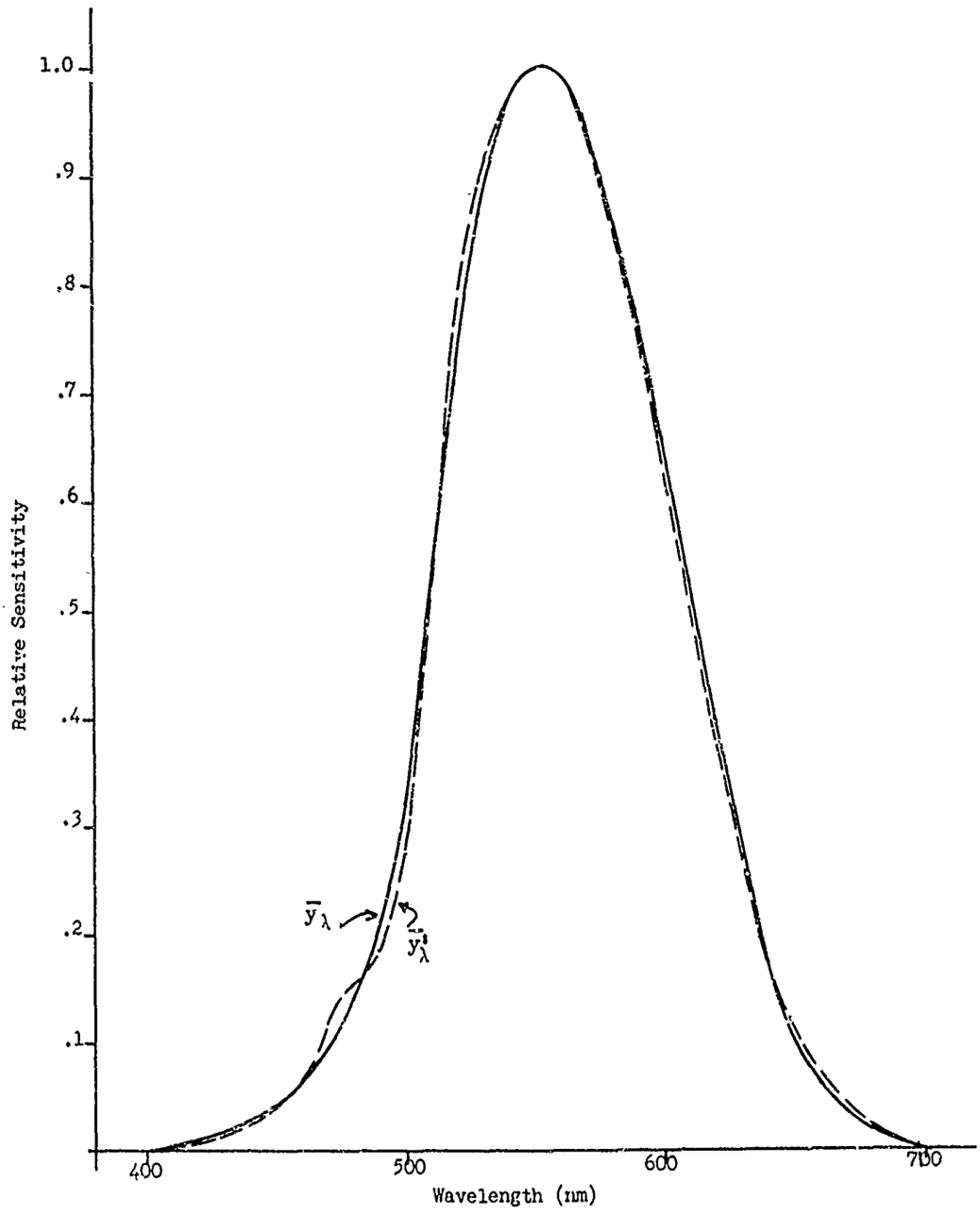

Fig 8 Relative spectral response of the new corrected silicon sensor vs the ideal $\bar{y}$ function

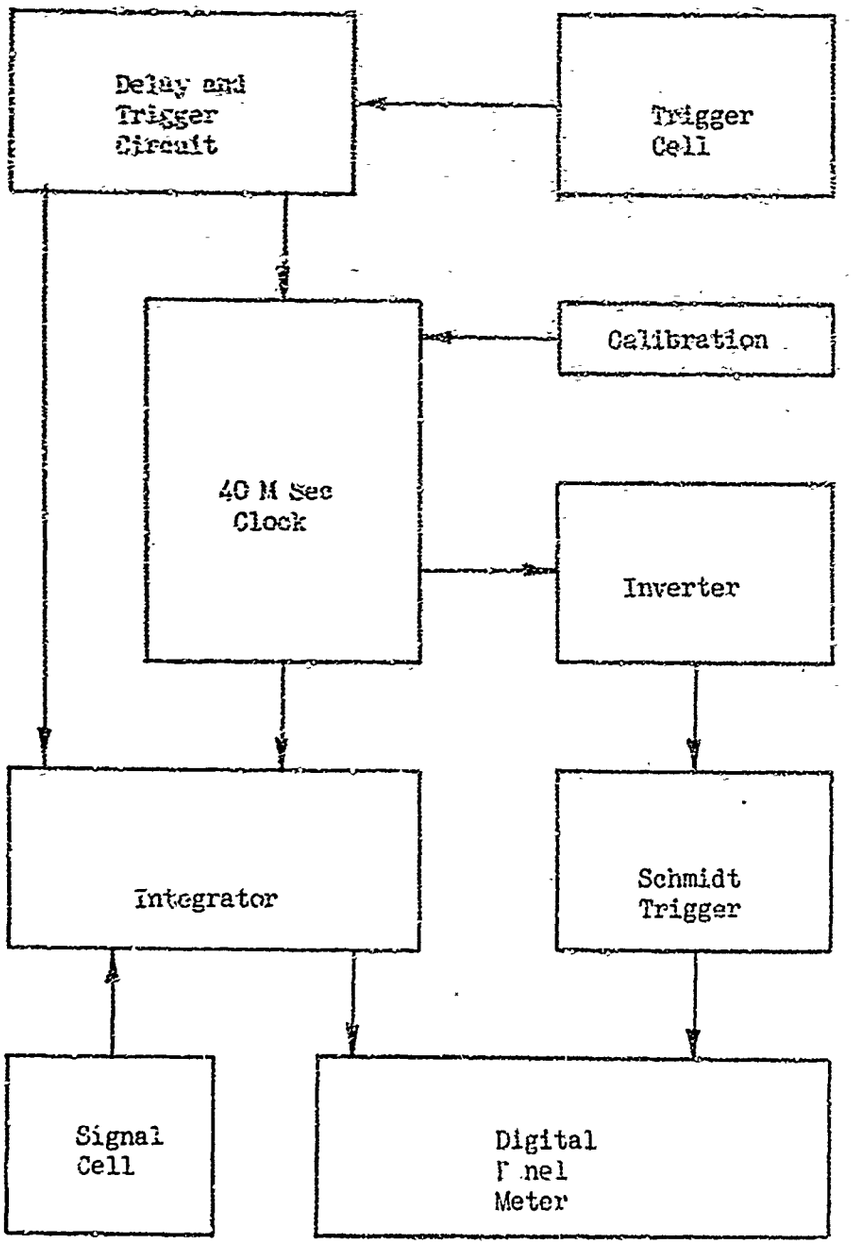

Fig 9 Block diagram of the analog integrator system

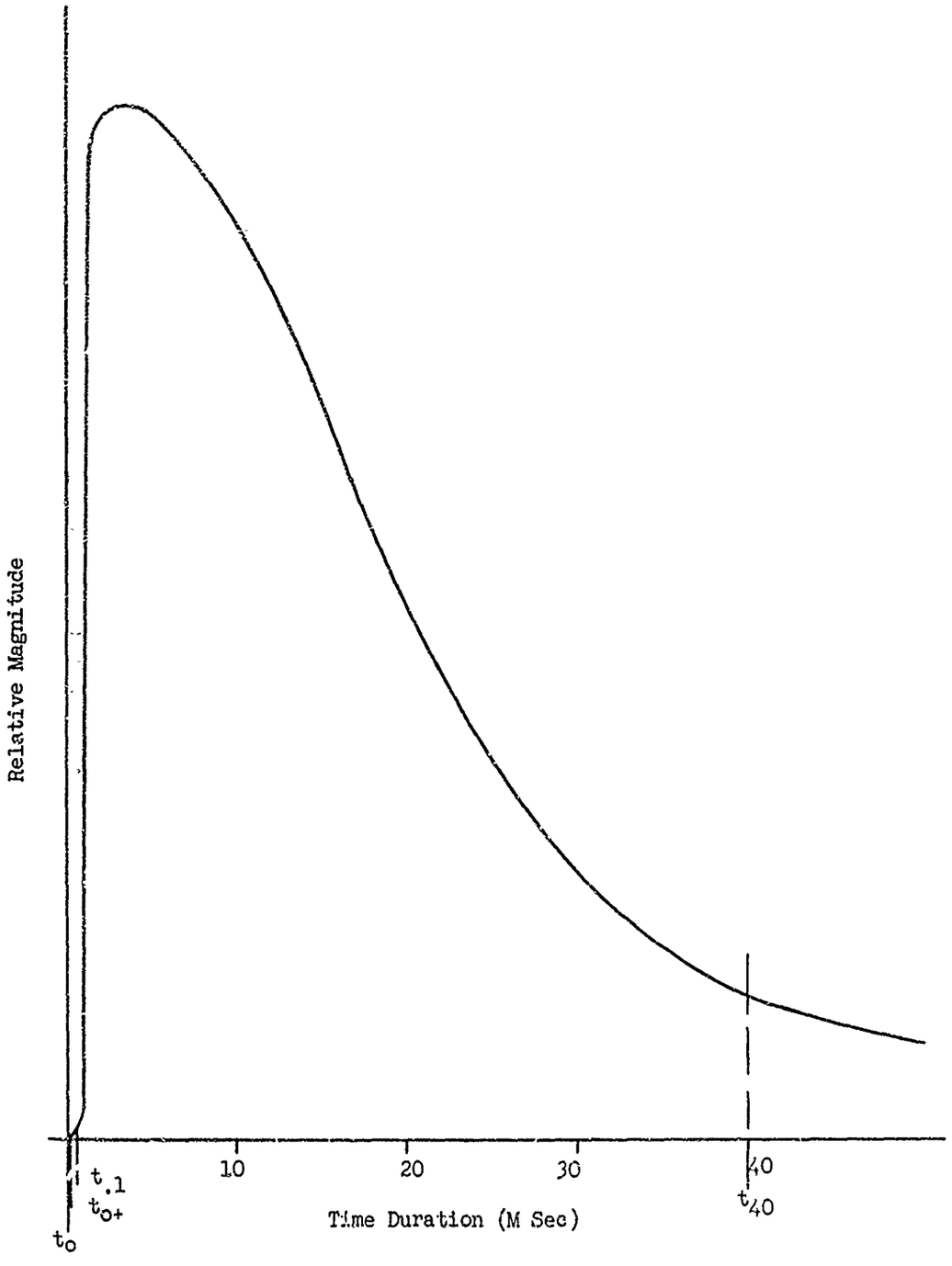

Fig 10 The light output of a typical photoflash

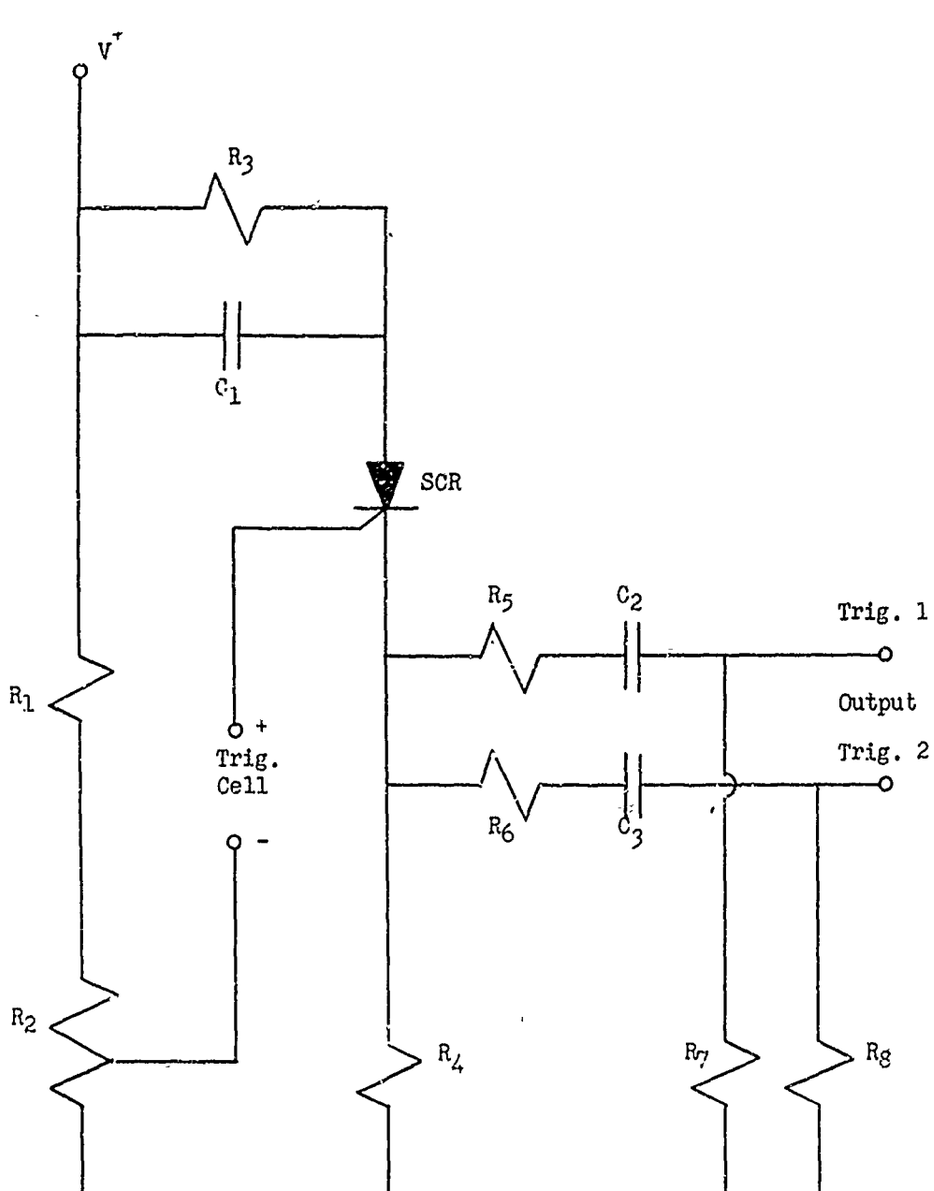

Fig 11 Trigger circuit for the digital panel integrator

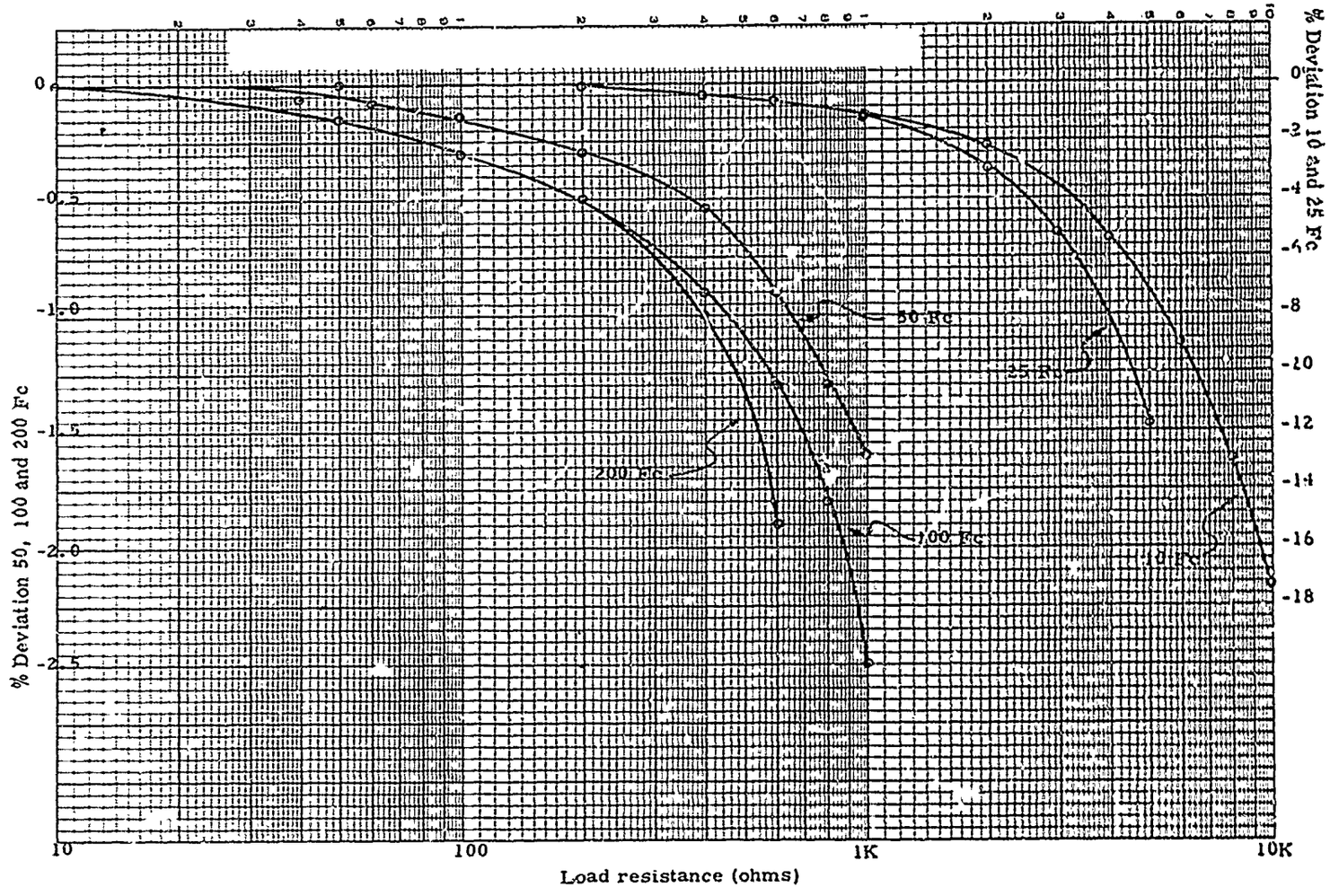

Fig 12 Linearity curves of silicon photocells vs light level and load